Supramolecular Aggregates as Templates: Ordered Mesoporous Polymers and Carbons†

Ying Wan,‡ Yifeng Shi,§ and Dongyuan Zhao*,§

Department of Chemistry, Shanghai Normal University, Shanghai 200234, P. R. China, and Department of Chemistry, Shanghai Key Laboratory of Molecular Catalysis and Innovative Materials, Fudan University, Shanghai 200433, P. R. China

Received August 25, 2007. Revised Manuscript Received September 24, 2007

Supramolecular aggregate's self-assembling approach has derived diverse mesostructured inorganic solids. Recent progresses involve ordered mesoporous carbonaceous frameworks. This review paper summarizes the synthesis of ordered mesoporous polymers and carbons based on the supramolecular aggregates as templates. Block copolymers are mainly introduced here. Both the aggregates of block copolymers themselves and the assembling with thermosetting resins have the abilities to organize ordered mesostructures. The understanding of the synthesis is on the formation of supramolecular arrangement of molecules, templating, cross-linking, removal of templates, and carbonization. In addition, the morphological control and the functionalization of ordered mesoporous carbonaceous materials are briefly summarized. The attractive mesoporous carbonaceous materials offer great opportunities in catalysis, water purification, electrodes, adsorbents, gas storage, aero-space, etc.

1. Introduction

The essence for the construction of ordered porous materials is the self-assembly in which molecules (or parts of molecules) spontaneously organize stable, structurally well-defined aggregates (in nanometer length scale).[1] Through utilization of the self-assembling approach, a family of ordered mesoporous solids with pore size ranging from 2 to 50 nm emerged in the early 1990s.[2,3] The aggregates come from the cationic, anionic, and nonionic surfactants, neutral amines, block copolymers, or their mixtures. They are disordered on the atomic or molecular scale but display periodical mesoscopic structure.[4,5] Supramolecular aggregates pack into three-dimensional (3D) ordered mesostructures according to the corresponding symmetries. At the final stage, the aggregates are removed by calcination, extraction, microwave digestion, oxidative decomposition, etc. Pores are opened, with the dimension, shape, and topology depending on the size and structure of supramolecular aggregates.[6–14] Both the interactions inside the surfactant molecules and between surfactants and framework components exhibit active significance to the assembly of ordered mesoporous materials. Diverse compositions have then been successfully synthesized, e.g., silicates, metals, metal oxides, sulfides, phosphates, and borates.[15–19]

Carbon can bond with itself principally via sp^3 (diamond-like) and sp^2 (graphitelike) covalence linkages. This unique ability leads to diversified molecular configurations including considerably attracted nanotubes and fullerene.[20] Porous carbons (mainly activated carbons, carbon blacks, carbon fibers) are widely used as adsorbents, gas storage materials, separation membranes, catalyst–supports, and electrode materials in fuel cells and electrochemical double layer capacitors (EDLC), because of large specific surface areas and pore volumes, chemical inertness, good mechanical stability, and low cost.[19,21] However, the practical applications of these porous carbons are restricted, such as adsorption of large molecules (organic dyes and biomolecules), chromatographic separation, and lithium ion cells, because of the limitation of the micropore size (<2 nm). Fast mass-transfer rate in larger pores are desirable. On the other hand, mesoporous polymers with large surface areas and pore volumes as well as unique organic frameworks, which can be easily functionalized, offer great opportunities in biological reactors, sensors, selective membranes, microelectrophoretic cells, heat insulators, catalyst–supports, etc.[22,23] Mesoporous carbons and polymers that have pore sizes between 2 and 50 nm therefore inspire tremendous research efforts.

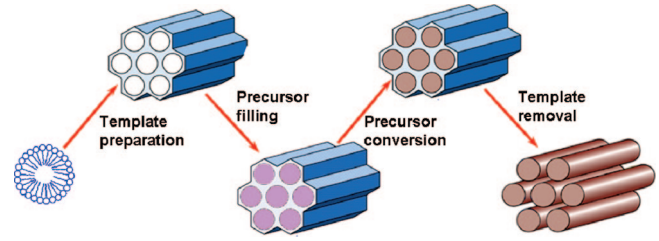

Figure 1. Schematic illustration for the nanocasting strategy.

Ordered mesoporous carbons and polymers are generally fabricated by a hard-templating approach (Figure 1).[19,24–26] In 1999, ordered mesoporous carbons were synthesized by Ryoo's and Hyeon's groups, respectively.[27,28] Mesoporous silicates derived from the surfactant self-assembly approach were used as the hard templates. After the incorporation of

† Part of the "Templated Materials Special Issue".

* To whom correspondence should be addressed. Tel: 86-21-5566-4194. Fax: 86-21-6564-1740. E-mail: dyzhao@fudan.edu.cn.

‡ Shanghai Normal University.

§ Fudan University.

10.1021/cm7024125 CCC: $40.75 © 2008 American Chemical Society
Published on Web 12/27/2007

carbon sources inside the mesopores, the composites were carbonized. Removal of the silica scaffold resulted in ordered mesoporous carbon replicating the silica mesochannels. The distinct advantage for the nanocasting process is the avoidance of organic surfactants as structure-directing agents (SDAs) and the hydrolysis and condensation process of precursors. Variable carbon precursors, e.g., sucrose, furfuryl alcohol, naphthalene, mesophase pitch, C_2H_2, polyacrylonitrile, and phenolic resin, can be utilized. The resultant mesostructures include $I4_132$, $Ia\bar{3}d$, $p6mm$ and $Im\bar{3}m$, and the macroscopic morphologies vary from film, rod, sphere, and "single crystal" to monolith.[24–26] However, these mesoporous carbons are constructed by amorphous carbon rod (wire) nanoarrays (only a few cases are partially graphitized).[24–26] Mesochannels are produced by the voids between carbon rods. Therefore, the pore size distribution is relatively wider than the mother silica template. In addition, the use of mesoporous silica as a scaffold makes the process expensive, complicated, and time-consuming, and in turn, unsuitable for the large-scale production and industrial applications.

Traditionally, the direct synthesis of mesoporous carbons include the catalytic activation of carbon precursors in the presence of metals and organometallic compounds, the carbonization of polymer blends with thermally unstable components, and the carbonization of polymer aerogels such as resorcinol-formaldehyde resins. Most of these mesoporous carbons possess relatively wide pore size distribution. On the consideration of the preparation methods for ordered mesoporous silicates, polymer aerogels have the possibility of being utilized as a precursor for the construction of ordered mesoporous carbon frameworks. This process involves organic sol–gel chemistry that is similar to that for silicates.[29] The control on the interactions between polymer aerogels and templates may direct the ordered mesoporous polymers and carbons. This strategy is of great importance because it can simultaneously get the organic and carbon frameworks. Moreover, the successful experiences in the production of mesoporous silicates can be referred, leading to the industrial progress on the manufacture for ordered mesoporous carbonaceous materials. However, when resorting to the supramolecular aggregates as templates in the synthesis of mesoporous carbonaceous materials, the challenge remains because of the high formation energy of C−C bonds. This review paper will summarize the efforts on the synthesis of ordered mesoporous polymers and carbons based on the supramolecular aggregates as templates. The attempt at understanding the synthesis is mainly on the basis of the synthetic procedure for mesoporous silica and the carbon chemistry: (1) formation of supramolecular arrangement of molecules. (2) templating. (3) cross-linking. (4) removal of templates. and (5) carbonization. Recent progress in the morphological control of ordered mesoporous carbonaceous materials is briefly summarized. In addition, the carbon-, or polymer-based nanocomposite materials and functionalized mesoporous carbons are also introduced mainly on the consideration of the reactivity of phenolic resin frameworks.

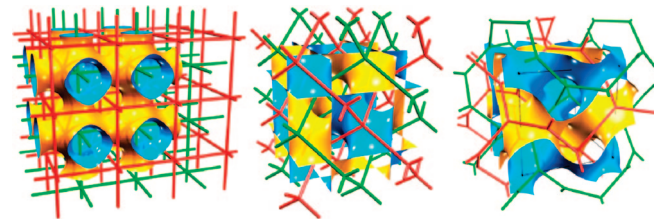

Figure 2. Bicontinuous cubic mesophases. From left to right: 3D periodical minimal P, D, and G surfaces. The rod connections display the channel directions. Reprinted with permission from ref 5. Copyright 2001 Wiley.

2. Liquid-Crystal Mesophase

Ordered mesostructures mainly depend on the ordered aggregates of amphiphilic surfactants. The liquid-crystal mesophase is the ordered supramolecular aggregates, coming from amphiphilic surfactants, block copolymers, graft copolymers, etc.[4,5] Amphiphilic surfactants contain a polar, hydrophilic headgroup and nonpolar hydrophobic tail(s). In solution, these supramolecules self-assemble to give ordered structures of various morphologies. These mesophases have different dimensions, charged characters, and liquid-crystalline domains. Here, we focus on the morphology of ordered liquid-crystal mesophase, skipping over the disordered packing.

Liquid-crystal mesophase can be mainly divided into lamellar, bicontinuous, mesh, columnar, and globular phases.[5]

(1) Lamellar mesophases (plannar, parallel stacks of amphiphilic bilayers). The mesophases include smectics, L_α, and L_β phases. Lamellar mesophases are the most commonly encountered mesophases. If the synthesis is not well-controlled, the unstable and unexpected lamellar mesostructure is the product.

(2) Bicontinuous mesophases (cubic warped bilayers). On the basis of the periodic minimal surface, this kind of phases includes P, D, and G cubic bicontinuous mesophases. Figure 2 shows the morphology and topological representation. The P-mesophase possesses the $Im\bar{3}m$ or $Pm\bar{3}m$ symmetry, and the topology (bilayer "open-cell foam") belongs to the bicontinuous α polonium structure ($4^{12}6^3$ net). This mesophase has not been achieved in the mesoporous family because of the unique bilayer structure. The symmetry for the D mesophase can be $Pn\bar{3}m$ or $Fd\bar{3}m$. Bicontinuous diamond structure (6^6-a) can give a representation of the so-called D surface. The minimum D surface mesostructure has been synthesized for mesoporous silica,[30] but not for the carbonaceous case yet. The symmetry and the topology of the G mesophase can be $Ia\bar{3}d$ or $I4_132$, and bicontinuous strontium silicide ($SrSi_2$), respectively. Fortunately, the helical bicontinuous mesostructures are common members in both mesoporous silica and carbonaceous materials.[9,31] These three bicontinuous mesophases with high symmetries can sometimes transform to low-symmetry ones, retaining the similar morphology. Bates and co-workers found the coexistence of bicontinuous $Ia\bar{3}d$ (Q^{230}), $I4_132$ (Q^{214}), and $Fddd$ (Q^{70}) phases in the liquid-crystal phase of poly(isopropenyl)-poly(styrene)-poly(ethylene oxide) (PI-PS-PEO).[32] Similarly, we observed that the bicontinuous cubic $Ia\bar{3}d$ carbon mesostructure partially transformed to the low $I4_132$ symmetry in some small domains upon carbonization.[31]

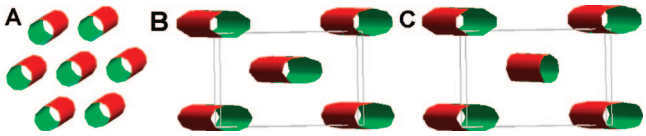

Figure 3. (A) 2D hexagonal closed packing of cylindrical micelles. (B) 2D rectangular packing of elliptical cylinder micelles. (C) Slant packing of elliptical cylinder micelles. Reprinted with permission from ref 5. Copyright 2001 Wiley.

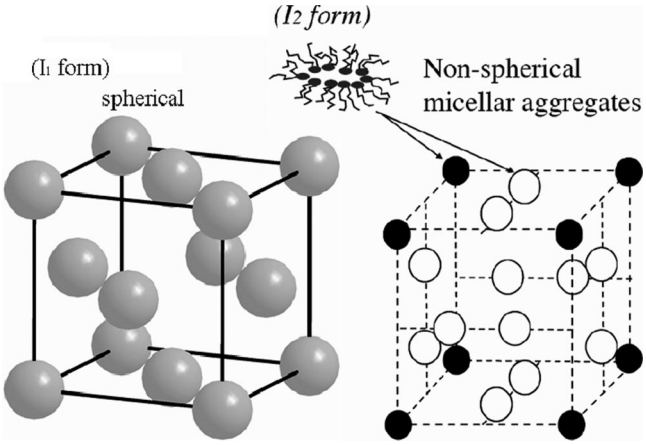

Figure 4. Discrete micellar (globular) mesophases: I1 (left) and I2 (right) form. Reprinted with permission from ref 5. Copyright 2001 Wiley.

(3) Mesh mesophases (stacks of rhombohedral, tetragonal perforated bilayers). The mesh mesophases have tetragonal (space group $R\bar{3}m$) and rhombohedral (space group $I422$) symmetries.

(4) Columnar mesophases (hexagonal/rectangular 2D lattices of rod micelles). Cylindrical micelles aggregate into a 2D hexagonal mesophase with the *p6mm* symmetry, which consists of H1 and H2 (inverse micelles) types. The mesostructure with the *p6mm* symmetry is the most common and easily formed one.[10,13,33] The elliptical cylinder micelles with 2D rectangular packing displays *cmm* symmetry. The anisotropy of micelles causes a slant packing, and hence, the space symmetry lowers to *pgg* (Figure 3). These low symmetrical mesostructures are rare for mesoporous materials; there are only a few examples for mesoporous silicas under very limited conditions.[9]

(5) Globular mesophase (discrete cubic, hexagonal packing of globular micelles). Discrete micelles contain two types: I1 and I2, corresponding to the closed packing of spherical micelles, and quasihomogeneous 3D Euclidean crystalline packing, respectively (Figure 4). The symmetries include $Im\bar{3}m$, $Fm\bar{3}m$, $P6_3/mmc$, and $Pm3n$. All symmetries have appeared in mesoporous silica series, but only the first two in mesoporous carbons.[9]

3. Self-Assembling Mesoporous Polymers and Carbons

3.1. Electrostatic Interaction. To yield mesoporous materials, it is important to adjust the chemistry of the surfactant head groups that can fit the requirement of the precursors.[9,12] Resorting to the first synthesis of ordered mesoporous silicates, the electrostatic interaction between the silicate precursor and the positively charged surfactant micelle leads to a supramolecular assembly.[3,10] In 1999, Moriguchi et al.[34] demonstrated the synthesis of lamellar and disordered polymer mesophases on the basis of the phenol-fomaldehyde resins and cationic surfactant assembly. An electrostatic interaction between the cationic surfactant and the negatively charged phenolic oligomers (under basic conditions) was proposed to form the micelle/polymer composite mesophase. The disordered mesostructure undergoes destruction upon the removal of cationic surfactants.

In alkaline media, oxidized polycondensed aromatic hydrocarbons from mesophase pitch with oxygen-containing groups, such as carboxyl, ether, phenol, or carbonyl, are soluble and display negative charges. This precursor can interact with the cationic surfactant through electrostatic force.[35] It should be noted that the precursor fragments are the small broken species from polyaromatic molecules. Coassembly of cationic surfactant and small oxidized polycondensed aromatic hydrocarbons leads to a wormlike mesostructure,[35] possibly because of the nonuniform precursor species and uncontrolled polymerization.

Resorcinol-formaldehyde aerogels that are prepared by an organic sol–gel process have been widely used as an intermediate to produce mesoporous carbons.[29] A surfactant-templating approach is natural to combine with this precursor. In fact, in the initial reports for mesoporous carbons, resorcinol-formaldehyde is the mostly adapted precursor. The polymerization of resorcinol and formaldehyde is extremely fast and difficult to be controlled even at room temperature. Many factors, such as resorcinol/formaldehyde ratio, catalyst content, pH value, temperature, etc., show great influence on the polymerization.[29] As a result, cationic quaternary ammonium surfactant self-assembly induces the disordered resorcinol-formaldehyde/surfactant mesophase.[36,37] Mesoporous carbon products from the surfactant template varies to a large extent, with the pore size ranging from 0.5 to >60 nm.

Disordered mesostructures are the majority products from the assembly of ionic surfactants and polymer precursors through the electrostatic interaction. Besides the uncontrolled polymerization of organic precursors, the main reason may be the extremely weak interaction between organic polymer frameworks and amphiphilic cationic surfactants. The charge density of ionic surfactant is not large enough to attract the carbon precursors, for example, phenolic resins by coulomb force for the ordered assembly. It results in the reduction of miscibility between organic frameworks and surfactants after the polymerization and consequent macroscopic phase separation.

3.2. Compatibility between Block Copolymers and Precursors. On the basis of the synthesis of mesoporous ceramics, we know the long PEO chains of amphiphilic triblock copolymers PEO-PPO-PEO are miscible with silicates and partially occlude into the silicate matrix.[38] Adding a PEO-compatible low-molecular-weight precured resin to an ordered PEO-containing block copolymer may result in an ordered mesostructure.[39] For example, the self-assembly of amphiphilic block copolymer poly(ethylene oxide)-poly(ethyl ethylene) (PEO-PEE) and poly(ethylene oxide)-poly(ethylene- *alt*-propylene) (PEO-PEP) and poly(bisphenol A-coepichlorohydrin)/phthalic anhydride epoxy resin leads

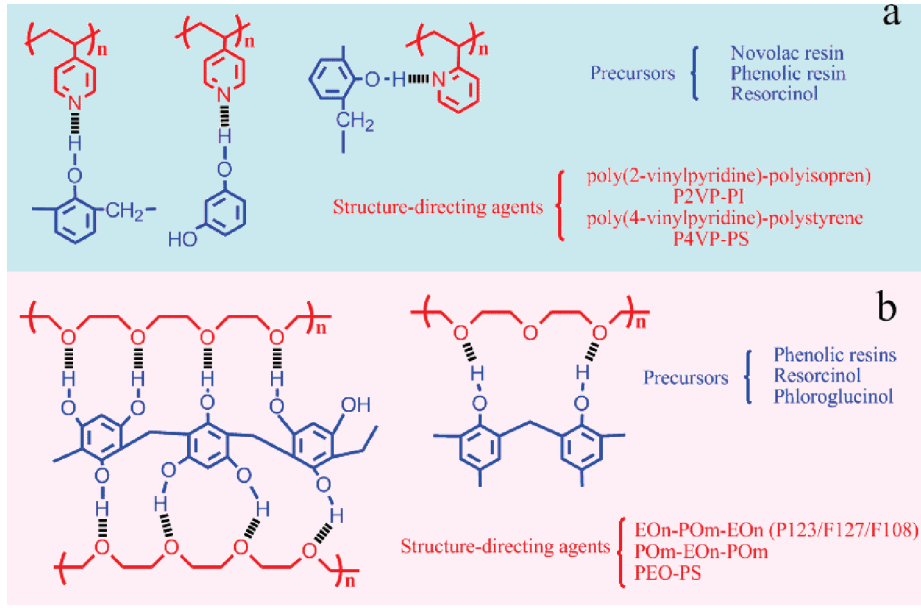

Figure 5. Hydrogen-bonding interaction between (a) pyridine-group-containing and (b) PEO-containing block-copolymers and the hydroxyl-group-containing organic precursors.

to the formation of well-defined morphologies upon solvent evaporation, including lamellar, cubic bicontinuous bilayers, hexagonally packed cylinders, and body-centered cubic-packed spheres. The dipole polarization between the PEO-PEP diblock copolymer and epoxy resin is strong enough to resist the phase separation due to the polymerization of resins, resulting in ordered morphologies. The various morphologies in one system can be explained by selective incorporation of the epoxy monomer in the PEO domains, which causes the PEO segments to swell. This causes an increased volume per PEO chain, whereas the volume per PEP chain remains unchanged. The change in the hydrophilic/hydrophobic ratio (V_H/V_L) contributes the variation of the curvature at the PEO/PEP interface, inducing the phase transformation.[39] Self-assembly and polymerization are separated and induced by the solvent evaporation. This approach skillfully avoids the cooperatively assembling process between the precursor and amphiphilic surfactant template, which facilitates the organic–organic self-assembly. Unfortunately, the block copolymer templates in the composites were not removed, possibly because of the small difference in the chemical and thermal stability between block copolymers and epoxy resins.

Hydrogen-bonding interaction between the template and the precursor is an efficient route to prepare mesoporous ceramics.[11,13] The interaction occurring on multisites and the compatibility are important mechanic features for the block-copolymer templating approach. Figure 5 represents the established hydrogen-bonding interactions between pyridine-group-containing and PEO-containing block copolymers with hydroxyl-group-containing organic precursors.

Ikkala and co-workers found that the self-assembling thermosetting resin can be derived from a system containing strongly hydrogen-bonded amphiphilic block copolymer and thermosetting precursor.[40–43] The pyridine groups of poly(2-vinylpyridine)-poly(isoprene) (P2VP-PI) diblock copolymers strongly interact with novolac phenolic hydroxyl groups.[40] Spontaneously, the nonpolar PI blocks get microphase separation from the blends of the miscible hydroxyl groups and P2VP blocks. By varying the fractions of PI blocks, the self-organized mesostructure can be tuned from lamellar to cylindrical and spherical phases. However, the network is unstable. Polymerization-induced phase separation may destroy the mesostructure.[40] It is the large molecular weight and linear feature of novolac phenolic resin that may be responsible for the poor self-organization. The polymeric framework cannot be annealed before the cross-linking took place. Enhancing the hydrogen-bonding interaction between the block copolymer (poly(4-vinylpyridine)-polystyrene, P4VP-PS) and the organic precursor (phenolic resin) avoid this destruction and maintain the ordered pore alignments.[43] Phenolic hydroxyl groups are strongly hydrogen-bonded to nitrogen in P4VP blocks, whereas PS blocks self-organize into hexagonally packed cylinders. Hydrogen bonds are strong enough to preserve the self-assembled mesostructure during the curing. When the weight fraction of PS segment is 60%, lamellar mesophase could be obtained. After pyrolysis at a temperature of 420 °C, nanoflakes are the products.[44] If the PS segment fraction reduces to 40%, the self-assembled mesostructure consists of periodic PS cylinders in the P4VP-phenolic resin matrix (Figure 6).[43] Pyrolysis at 420 °C can degrade the diblock copolymer, giving open cylindrical pores. However, the polymeric matrix is thermally unstable, perhaps because of the lack of the 3D interconnecting sites of the linear novolac phenolic resin. Prolonging the heating time to 120 min may partially destroy the ordered pore alignment.

Dai and co-workers developed the enhanced hydrogen-bonding interaction between the pyridine group and resorcinol or between ethylene oxide and phloroglucinol in the synthesis of highly ordered mesoporous carbons.[45,46] A thin film containing hydrophilic P4VP and resorcinol domains and hydrophobic PS domains self-assembles an ordered hexagonal mesostructure (Figure 10).[45] The swelling role of resorcinol in hydrophilic domains induces the order−order

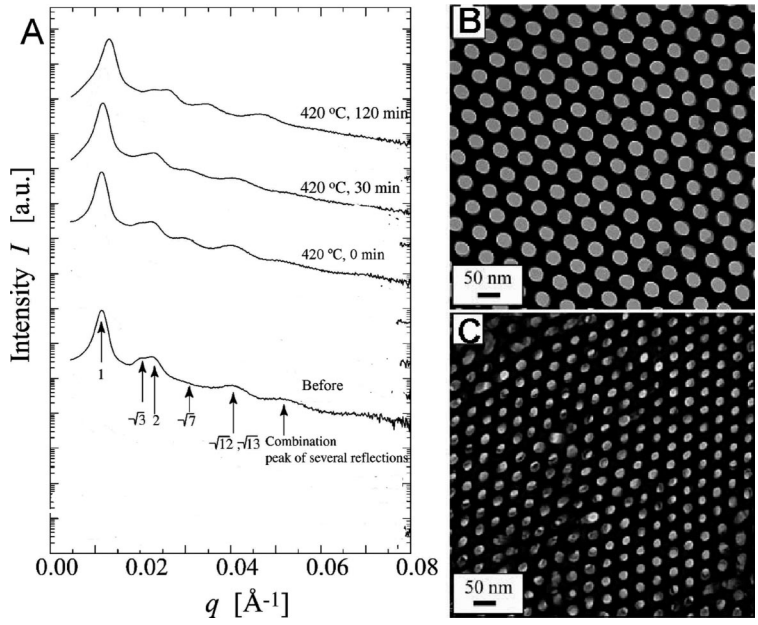

Figure 6. (A) SAXS patterns for the cured phenolic-resin-P4VP-PS composites before and after pyrolysis at 420 °C for different time. (B, C) TEM images of the mesoporous phenolic-resin pyrolyzed at 420 °C for (B) 30 and (C) 120 min. A partial collapse of the pores is observed in (C). Panel A was replotted to reduce several lines for simplification. Reprinted with permission from ref 43. Copyright 2007 Wiley.

phase transition from lamellar to columnar mesophase (the PS domain weight fraction of about 35% in the composite). The sufficient repulsion between the PS domains and the P4VP/resorcinol domains favors the reserve of the highly ordered alignment together with the enrichment of resorcinol in the matrix upon solvent evaporation. Polymerization is then carried out by exposing the thin film to formaldehyde vapor. These steps restrict the condensation of resorcinol and formaldehyde in a confined space, or in other words, around block copolymer aggregates. The matrix is highly cross-linked with a minor influence on the ordered structure. After carbonization at 800 °C, mesoporous carbon thin film possesses oriented cylindrical pores perpendicular to the substrate with dimensions of 33.7 ± 2.5 nm (Figure 7). The CVD technique is applied, and the operation is complicated and unsuitable for the large-scale production. Less-ordered mesoporous carbon thin films were obtained from the phloroglucinol/formaldehyde/PEO-PPO-PEO system. The possible reason is that the condensation rate of phloroglucinol and formaldehyde is too fast to be controlled during the fast formation of thin films.

On the basis of the thermosetting resorcinol/formaldehyde resins, ordered mesoporous carbon thin films (COU-1) have also been synthesized by Tananka et al. via the triblock copolymer F127-templating route.[47] The addition of triethyl orthoacetate (EOA) as a cocarbon source is necessary, possibly because it can reduce the condensation rate of resorcinol and formaldehyde to some extent. An overly fast condensation rate would result in self-polymerization of resins instead of alignment around the amphiphilies. FE-SEM images of COU-1 show that the pores are parallel to the film surface and a periodic mesostructure consists of hexagonally arranged pores (Figure 8). However, the resultant mesoporous carbons display only one strong XRD diffraction peak and relatively irregular N_2 sorption isotherms. These phenomena imply that the mesostructure could not be resolved. In addition, the ordered carbon mesostructure may undergo partial collapse during the high-temperature carbonization.[48]

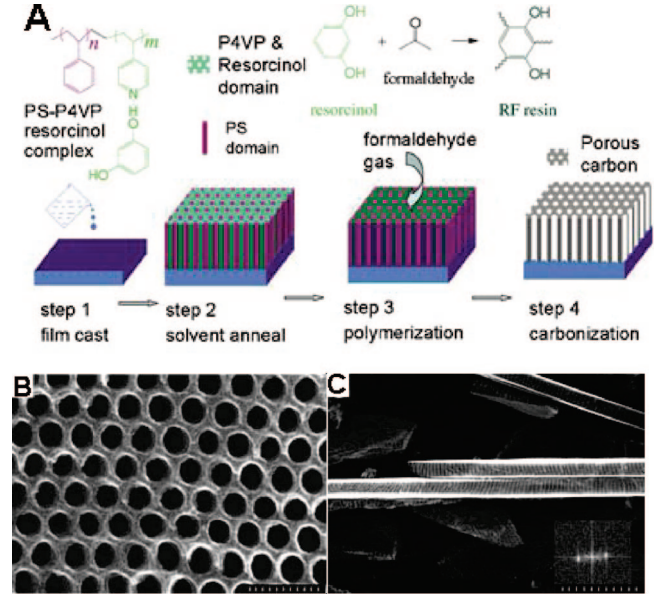

Figure 7. (A) Schematic presentation of mesoporous carbon obtained from the organic–organic self-assembly of resorcinol/formaldehyde and diblock copolymer PS-P4VP. (B) High-resolution SEM image of the surface of the carbon film. (C) SEM image of the film cross-section. The inset is the FT of the cross-section image. The scale bar is 100 nm for each image. Reprinted with permission from ref 45. Copyright 2004 Wiley.

Recently, on the combination of soft-matter chemistry and self-assembled mesoporous silicates, we independently developed the organic–organic self-assembly approach to a family of mesoporous phenolic resins and carbons with various mesostructures.[33,49–51] All materials involved in the synthesis are commercially available. Low-molecular-weight phenolic resol, which is polymerized from phenol and formaldehyde under basic conditions, first mixes with PEO-PPO-PEO triblock copolymer in an ethanolic solvent.[33,49]

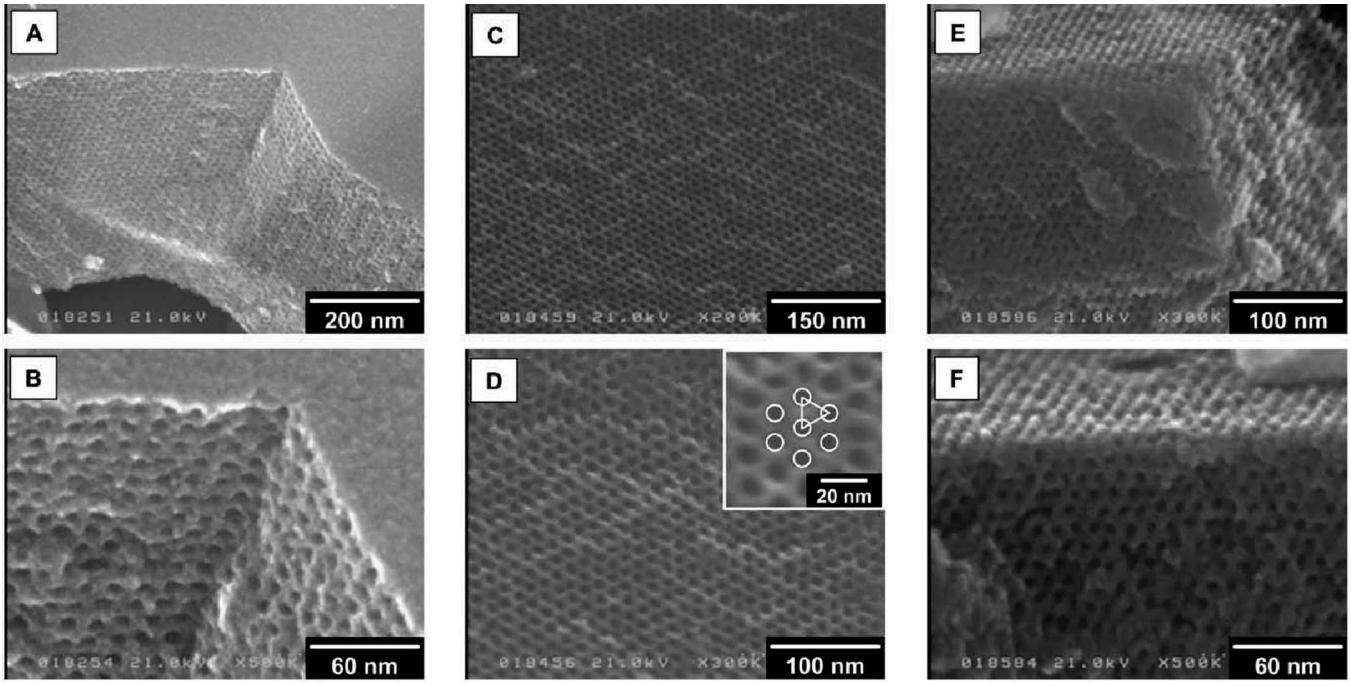

Figure 8. FE-SEM images of COU-1 after carbonization at (A, B) 400, (C, D) 600, and (E, F) 800 °C, respectively. Reprinted with permission from ref 47. Copyright 2005 Royal Society of Chemistry.

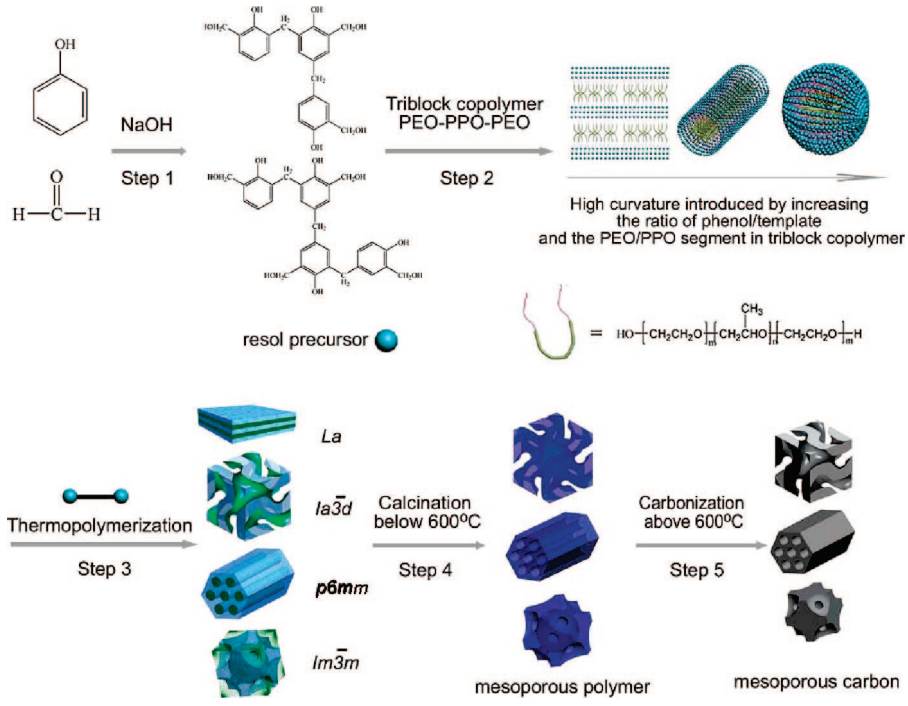

Figure 9. Scheme for preparations of ordered mesoporous polymer resins and carbon frameworks. Reprinted with permission from ref 49. Copyright 2006 American Chemical Society.

Evaporation of the solvent induces the self-assembly of the block copolymer to an ordered structure. Driven by the hydrogen-bonding interaction between the PEO block and phenolic resol, the ordered mesostructure of the phenolic resol/block copolymer composite is formed. Curing of the resol at 100 °C solidifies the polymeric framework. Because of the difference in chemical and thermal stability between the resin and triblock copolymer, the template can be removed either by calcination at 350–450 °C or by extraction with 48 wt % sulfuric acid solution, leaving the Bakelite framework with ordered aligned voids. Heating at a high temperature above 600 °C transforms the polymeric framework to homologous carbon mesostructures. Figure 9 illustrates the five-step synthesis procedure. The increase in both the resol/triblock copolymer ratio and the PEO content in triblock copolymers results in the swelling of the hydrophilic volume with the maintenance of the hydrophobic volume per block and, in turn, an increasing curvature at the PEO/PPO interface. Therefore, the enlargement of the hydrophilic/

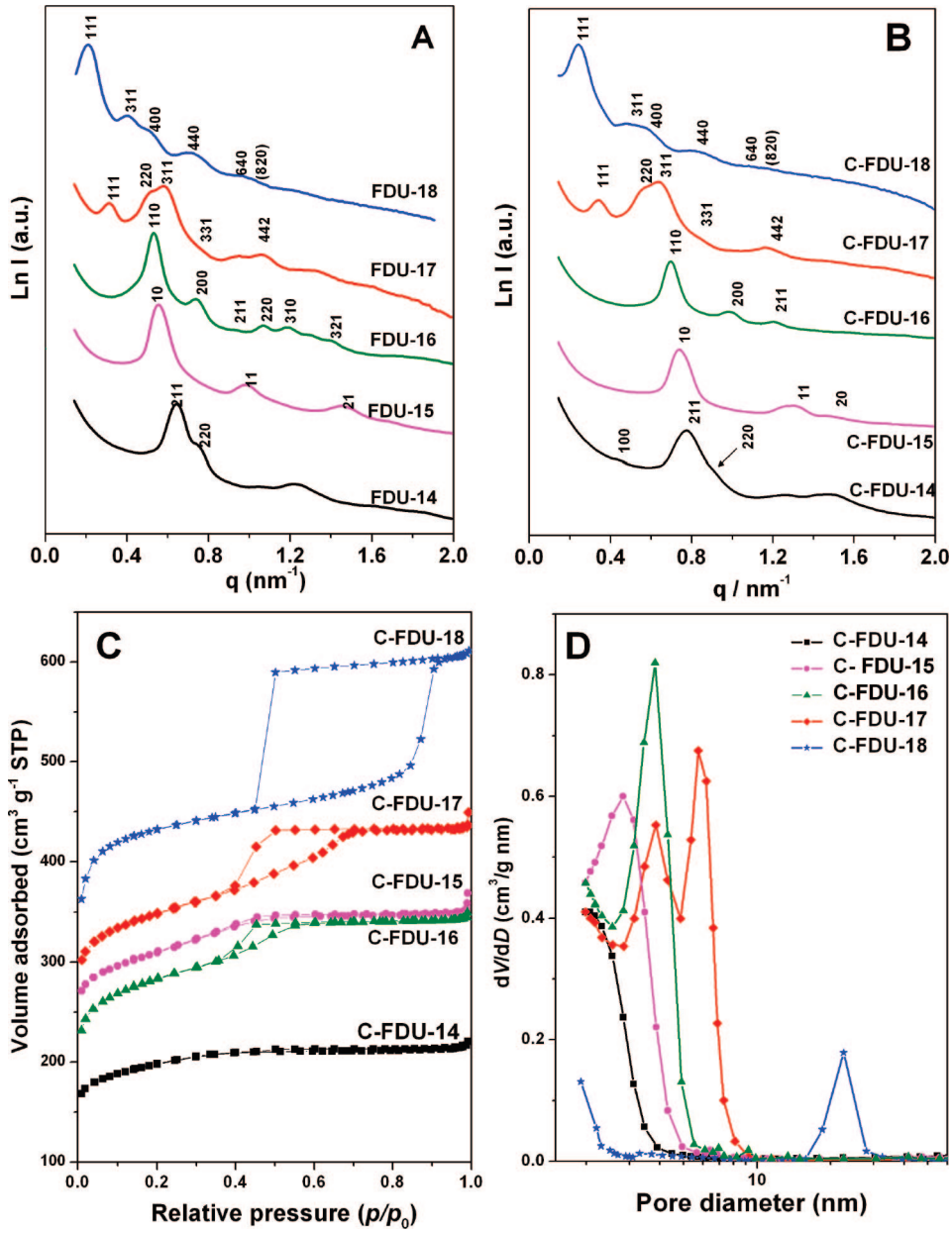

Figure 10. (A, B) SAXS patterns, (C) N_2 adsorption isotherms, and (D) pore size distributions of mesoporous polymer FDU- *n* (A) and mesoporous carbon C-FDU- *n* (B−D). The isotherms for C-FDU-17 are offset by 100 cm^3/g. $n = 14 - 18$, represents 3D gyroid $Ia\bar{3}d$, 2D hexagonal *p6mm*, 3D body-centered cubic $Im\bar{3}m$, 3D face-centered cubic $Fd\bar{3}m$, and 3D face-centered cubic $Fm\bar{3}m$ symmetry, respectively. The carbonization temperature for C-FDU-14, -15, -16, -17, and 018 is 800, 1200, 1200, 1000, and 900 °C, respectively. Reprinted with permission from refs 49−51. Copyright 2006 and 2007 American Chemical Society, and Copyright 2007 Wiley.

hydrophobic ratio in the triblock-copolymer-resols composite causes the mesophase transformation from lamellar, bicontinuous $Ia\bar{3}d$, columnar *p6mm* to globular $Im\bar{3}m$ mesophases. N_2 sorption isotherms show typical type IV curves, indicative of mesoporous materials with uniform pore size distribution. The pore dimension is about 7.0 and 4.0 nm for the mesoporous Bakelite and carbon, respectively. Mesoporous carbons have large surface areas (∼1500 m^2/g) and pore volumes (∼0.85 cm^3/g). It is featured that the carbon mesostructures are highly stable and can be retained at a temperature as high as 1400 °C under a nitrogen atmosphere.[33] Partial results are shown in Figure 10. Supported by this kind of ordered mesoporous carbon molecular sieves, platinum catalysts have highly dispersed and uniformly sized metal nanoparticles and exhibit good hydrogen electro-oxidation properties that show potential for electrodes in fuel cells.[52]

Following this concept, other PEO-containing block copolymers can also template the mesoporous bakelites and carbons to propagate the pore structures and dimensions. A two-component mixture of laboratory-made, large-molecular-weight PEO-PS block copolymer (PEO_{125}-PS_{230}) and low-molecular-weight phenolic resin assemble to ordered morphologies.[51] Discrete cubic packed spheres of PS blocks (or in majority) in a matrix of the long-chain PEO block and resin are formed. The pore alignment is dependent on the packing of discrete micelles, belonging to the face-centered cubic $Fm\bar{3}m$ mesosphase. Ordered mesoporous phenolic resins and carbons are the products after the removal of the diblock copolymer template and

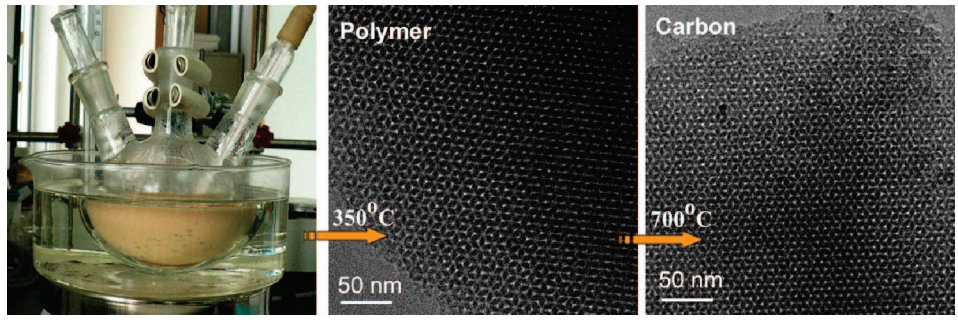

Figure 11. From left to right: photo of a typical apparatus for the cooperative assembly of phenol-formaldyde-P123 in a dilute aqueous solution; TEM image of the mesoporous polymer after calcination at 350 °C; TEM image of the mesoporous carbon after carbonization at 700 °C. Reprinted with permission from ref 31 Copyright 2005 American Chemical Society.

carbonization. The pore size depends on the length of hydrophobic PS blocks. N_2 sorption isotherms reveal a large mesopore with the dimension of 22.6 nm due to the large molecular weight of the PS block (Figure 10). In addition, the long segment of PEO blocks facilitates the formation of interconnected microtunnels between the isolated spheres after the pyrolysis of the diblock copolymer. The mesopores that are connected by microtunnels are accessible by N_2 molecules. This phenomenon is in contrast to the silica mesostructure that is made of isolated and closed silica spheres.[53] The latter shows no porosity. A selective swelling of the PEO phase with phenolic resols can also be achieved in the reversed triblock copolymer PPO-PEO-PPO self-assembled structure.[50] The micellization of the reversed triblock copolymers is less favorable than that of triblock copolymers PEO-PPO-PEO and are seldom used in the synthesis of ordered mesoporous silicas.[54–56] Two outer PPO blocks in a chain participate in two different micelles or aggregates, forming interconnected micelles.[54–56] In a certain molar ratio, the mixture of reversed triblock copolymer PPO-PEO-PPO with large PEO weight fraction of 45% and phenolic resol self-assembles to face-centered cubic packed spheres of PPO blocks with the $Fd\bar{3}m$ symmetry in the PEO/phenolic resin matrix. A slight decrease in the phenolic resol/triblock copolymer ratio would lead to the formation of the 2D hexagonal mesostructure. Interestingly, highly ordered mesoporous polymer and carbon frameworks with the $Fd\bar{3}m$ symmetry have a bimodal pore-size distribution centered at 3.2–4.0 and 5.4–6.9 nm, respectively (Figure 10).

An industrially feasible dilute aqueous induced self-assembly strategy was demonstrated by our group.[31,57] The route is similar to that for mesoporous silicates. Precured phenolic oligomers (resols) and triblock copolymers are mixed in a weak basic aqueous solution. After the coassembly, solidification of the mesostructure, and removal of template and carbonization, mesoporous polymers/carbons are obtained (Figure 11). The successful coassembly is driven by one-layer H-bonding interaction. This is different with mesoporous silica, for which a double-layer H-bonding interaction is the driving force. Therefore, the assembling rate for phenolic resols and triblock copolymers is much slower than that for silicates. It takes more than 10 h to get the precipitation of the resol-triblock copolymer composites. The coassembly strongly depends on the phenol/base catalyst (NaOH) ratio. A high phenol/NaOH ratio leads to a poor polymerization of resols and, in turn, a failed assembly and condensation around the amphiphilic triblock copolymer aggregates. If the phenol/NaOH ratio is overly low, anionic resol precursors quickly polymerize under the relatively strongly basic conditions, resulting in a disordered mesostructure. A phenol/NaOH molar ratio of 4.0–4.2 with a pH value of 8.5–9.0 favors the formation of highly ordered mesoporous polymers and carbons. This aqueous cooperative assembly route shows the superiority in the industrial production. Besides that, it can expand pores. Similar to the assistance of trimethylbenzene (TMB) in synthesis of mesoporous silicates,[9] the use of hydrocarbons can swell the pores for mesoporous carbonaceous materials.[57] Although the pore-expansion role for hydrocarbons is limited, this route may provide an idea on tailoring the pores of mesoporous polymers and carbons.

Inherent to the surfactant templating approach, the interactions on surfactant/precursor species interfaces and inside species themselves play important roles on the polymer and carbon mesostructures. Several issues should be addressed:

(1) SDAs. Block copolymers with one block sufficiently compatible with a thermosetting resin and one other block sufficiently repulsive are good SDAs.

(2)Templating. The strong interaction between the SDAs and organic precursor is a key issue. Several cases have been shown here to highlight the importance for the strong hydrogen-bonding interaction in the preparation of ordered mesoporous carbonaceous materials. For example, highly ordered mesoporous polymers and carbons have been successfully synthesized in the system of low-molecular-weight basically catalyzed phenolic resols as precursors and PEO-containing block copolymers as templates. The precursors have plenty of hydroxyl and benzyl groups that can form strongly hydrogen-bonding interactions with amphiphilic block copolymers. Second, the precursors should be small enough to assemble around the amphiphilic block copolymer aggregates. The prepolymerization of polymeric oligomers is a choice to control the condensation of the monomers. Not only phenol/formaldehyde resol[49] but also resorcinol/formaldehyde resol,[48] which has a much higher condensation rate than the former, can assemble with the triblock copolymer if the prepolymerized oligomers are used as the precursor. Self-assembly of block copolymers induces the highly ordered mesostructure.

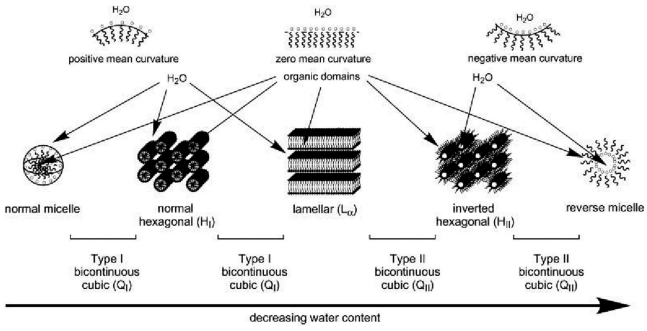

Figure 12. Schematic representation of an ideal progression of lyotropic liquid crystal (LLC) phases as a function of system composition and mean curvature. The various bicontinuous cubic phases exist between the illustrated LLC phases and micellar structures. Reprinted with permission from ref 58 Copyright 2003 American Chemical Society.

(3) Cross-linking. Curing the polymer fixes the framework. The polymeric framework should be rigid enough to resist the polymerization-induced macroscopic phase separation. Base-catalyzed condensation of phenol and formaldehyde results in phenolic resin of a "rigid" 3D network structure with benzene rings as three or four cross-linking sites. This kind of cross-linked structure is similar to that of covalently bonded silicate zeolite frameworks, in which one silicon atom is linked to four other silicon atoms through Si−O bonds. In contrast, linear novolac resin may lack this property, leading to an unstable framework.

(4) Template removal. The feature that the polymeric frameworks are more stable than block copolymers facilitates the elimination of templates with the maintenance of the mesostructure matrixes.

(5) Carbonization. The key point in this process is the assurance of the mesostructural stability. A uniform shrinkage is required. Therefore, pure inert carbonizing atmosphere such as nitrogen and argon is favorable. A small amount of oxygen in N_2 or Ar gas generates micropores in the carbonaceous pore walls. Similarly, the addition of CO_2 and H_2O in the carbonizing atmosphere could cause micropores. The temperature is generally above 600 °C. The carbonization under an atmosphere of 4% O_2 in N_2 at 700 °C would lead to the agglomeration of pore walls.

This simple, reproducible approach by self-assembling low-molecular-weight polymers and triblock copolymers opens an avenue to diverse polymer and carbon mesostructures that have great potentials in many high-tech applications.

4. Direct Synthesis

Ordered aggregates of amphiphilies themselves have the ability to produce ordered mesoporous polymers. This approach can be called a "nontemplating" method.

4.1. In situ Cross-Linkage of Micelles. The ordered domains of liquid crystals can be "fixed" by cross-linking of the amphiphilic molecules or block copolymers. For example, Gin and co-workers utilized polymerizable amphiphilic surfactants to assemble the ordered aggregates in aqueous solutions (Figure 12).[58] After the polymerization between the nearest neighbor head groups, several kinds of ordered mesostructured polymers have been fabricated, including lamellar, 2D hexagonal, and 3D cubic mesostructures.[58] Metal ions, which serve as catalysts, can be incorporated with the hydrophilic moieties and therefore confined inside the pores.[59] These sites offer good catalytic performance for these mesostructured polymers. However, the pore channels are occupied by water or solvent molecules, without accessible space.

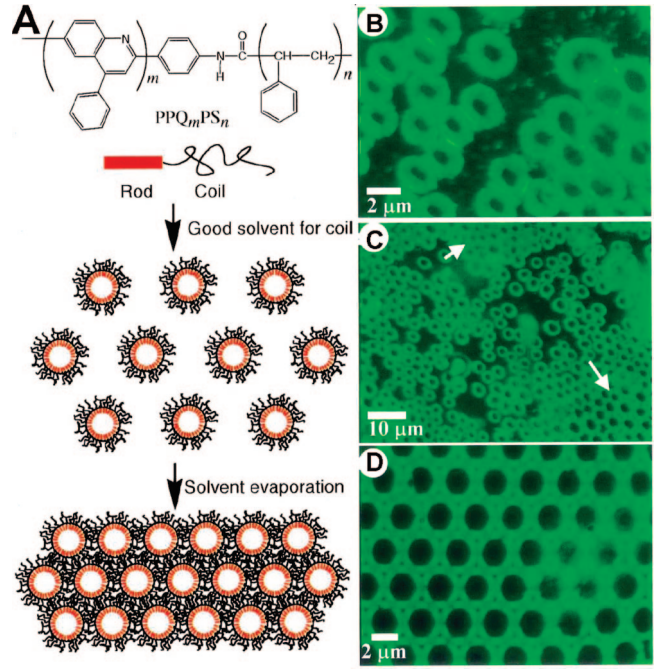

Figure 13. (A) Schematic illustration of the hierarchical self-assembly of rod−coil diblock copolymer PPQ-PS into ordered porous materials. (B−D) Fluorescence photomicrographs of solution-cast micellar films of (B) 0.005, (C) 0.01, and (D) 0.5 wt % PPQ-PS obtained by ambient air drying of diblock solutions in CS_2. Reprinted with permission from ref 60. Copyright 1999 Science.

Rod−coil diblock copolymers are attractive whose self-organization leads to the hollow spherical micelles in a selective solvent.[60] The discrete micelle consists of a hollow core, a rodlike inner shell, and a flexible-coil outer corona. For example, as shown in Figure 13, diblock copolymer poly(phenylquinoline)-polystyrene (PPQ-PS) in carbon disulfide (CS_2), which is a selective solvent for the PS block, generates hollow spherical micelles.[60] Upon solvent evaporation, the discrete micelles self-organize highly periodic mesostructures. Self-ordering of the rigid, rodlike blocks is the main driving force. The hexagonally arranged multilayers possess open pores, and the pore structure and dimension inherit from the diblock copolymer (molecular weight, length of each segment, etc.). However, the porous polymers are unstable because of the fact that the frameworks are constructed by van der Waals interaction. The pore size is about 1.5 μm, out of the range of mesopores.

4.2. Selective Etching of One Block in Ordered Aggregates of Block Copolymer. In this case, block copolymers first self-organize ordered mesostructures. If microphase separation occurs upon cross-linking of the block copolymer, namely, that one block packs and aligns in another block matrix, selective degradation of one block produces the continuous nanochannels.[23] Nakahama and co-workers first demonstrated this method.[61] A hexagonally packed array of polyisoprene (the minor component) cylin-

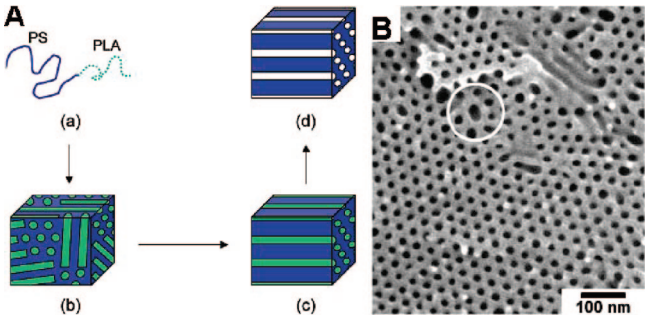

Figure 14. (A) Synthesis procedure of nanoporous polymers from diblock copolymer: (a) self-assembling of diblock copolymer PS-PLA to (b) a polydomained cylindrical morphology; (c) shear-aligning to a monolith; (d) hydrolytic removal of PLA to a nanoporous monolith. (B) Scanning electron micrograph of porous material from PS-PLA using this strategy, viewing perpendicularly to the cylindrical axes. A defect is encompassed by the circle. Reprinted with permission from ref 62. Copyright 2002 American Chemical Society.

ders in siloxane-functionalized polystyrene is formed from the PS−PI diblock copolymer. Siloxane serves as a cross-linking agent to immobilize the mesostructure. The PI blocks are removed from the cross-linked thin films through ozonolysis and nanopores are generated. Hillmyer and co-workers prepared polymer mesostructures from the self-assembly of polystyrene-polyactide (PS-PLA) block copolymers (Figure 14).[62] The PLA segment form hexagonally packed nanocylinders in the PS matrix, which is subsequently eluted by a basic methanol/water solution. Macroscopic alignment can be obtained by shearing stress. The shear-aligned polymer monolith possesses ordered mesostructure, large pore size, and highly aligned pores. A large number of hydroxyl groups is retained after chemical etching of PS blocks, which renders the polymer for further functionalization. The functionalization can also be achieved by adding a third segment in the ABC block copolymer, such as polystyrene-polydimethylacrylamide-polyactide (PS-PDMA-PLA).[63] Upon cross-linking of the polymer and elimination of the PLA blocks, nanoporous PS matrix contains hexagonally arrayed channels with the dimension of about 20 nm coated with PDMA. Inherent hydrolysis nature of the PDMA segment brings about carboxylic groups to the pore internal surface. ABC triblock copolymers also have the advantages in rich ordered microdomains and diverse components. The hydrophobic/hydrophilic properties and self-assembly of ABC copolymers strongly depend on the interaction factors (χ_{AB}, χ_{AC}, χ_{BC}) and the component factors (f_A, f_B). For instance, tuning the component factors in the poly(ethylene oxide)-poly(methyl methacrylate)-polystyrene (PEO-PMMA-PS) triblock copolymers in which PS is the major component and the other two are minor components, the assembly of the block copolymers provide highly ordered, defect-free nanoporous thin films.[64] This triblock copolymer shares the superiority of the high degree of lateral ordering for PS-PEO diblock copolymers and the facile degradability for PS-PMMA diblocks. Cylinder domains of the PMMA block separate from the core–shell morphology of PS-PEO diblock when the PMMA block is in a certain chain length. UV irradiation following by acetic acid rinsing efficiently degrades the PMMS block, resulting in the mesoporous polymer with a uniformly pore size distribution. The mesostructures such as Q^{214} ($I4_132$), Q^{230} ($Ia\bar{3}2$), and O^{70} ($Fddd$) structures are expected on the basis of the aggregating behaviors of ABC triblock copolymers. The problem of unstable polymer frameworks is also true in this case. No isothermal sorptions are available. Accordingly, BET surface areas are not given.

If the polymer matrix can be carbonized with the maintenance of the oriented texture, mesoporous carbon is the expected product. Self-ordering structure of a diblock copolymer with a carbonization-precursor block such as poly(acrylonitrile) (PAN) and a sacrificial block such as poly(*n*-butyl acrylate) (PBA) is obtained by microphase separation. After removing the sacrificial block and carbonizing the other block, nanoporous carbon is yielded.[65–67] Most products are carbonaceous thin films. The substrate supports the nanostructure to some extent. In addition, the mesostructure is less ordered, mainly because of the structural distortion and large shrinkage during carbonization.

5. Morphology Control

Practical applications require the various macroscopic morphologies, for example, uniformly sized spheres in chromatography, films in sensor and separation, transparent monoliths, and thin films in optics. Unlike conventional materials, the macroscopic morphologies of mesoporous solids are difficult to postprocess and shape. During the synthesis, mesostructure assembly and morphology growth should be concurrently controlled.[68] Different from mesoporous silicates, most polymer and carbon mesostructures are obtained by the EISA method. As a result, the research on the morphological control lags behind that for mesoporous silicas. Despite of this fact, the mesoporous polymers and carbons have been produced with different morphologies such as thin film,[45,47] membrane,[33] monolith,[46] fiber, 46 sphere,[69] rod,[57] single-crystal,[70] discus-like crystal,[70] etc.

The mesostructures obtained by the EISA method normally require substrates, such as silicon wafer, producing thin films or membranes.[33,45,47] The aerosol-assisted self-assembly route produces polydispersed mesoporous carbon spheres with diameters at the micrometric scale.[69] To get fibers with well-aligned mesopores, the shear-aligned block copolymer/polymeric matrix is used.[46] The phloroglucinol/Pluronic F127 complex reacts with formaldehyde to form a phenolic resin/F127 composite. Macroscopic alignment by shearing force such as spin coating and fiber extrusion produces mesostructured films and fibers. Flexible carbon sheets can be woven by the fibers (Figure 15).

The aqueous cooperative assembly route from phenol/formaldehyde and triblock copolymer (F127 and P123) under weakly basic conditions produces pelletlike mesoporous carbons in the size range of 1–5 mm, rodlike particles ranging from 5 to 200 μm, perfect rhombdodecahedral single crystals and discuslike crystals.[57,70] The match of the rate between the polymerization of resols and the growth of mesostructured crystals may be responsible for these phenomena. The PEO/PPO ratio and the concentration of triblock copolymers influence the hydrophilic/hydrophobic ratio of the mesophase, and in turn, the hydrogen-bonding interaction as well as the aggregation of polymer sediments. Large pelletlike particles

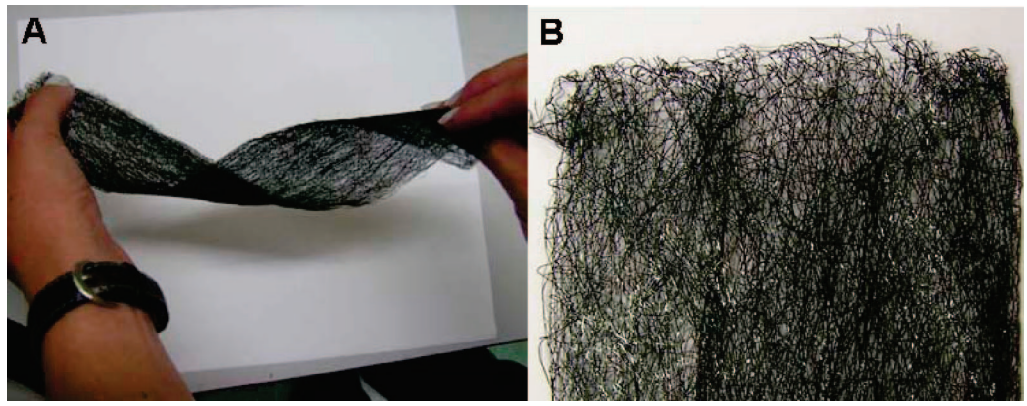

Figure 15. Photos of the flexible carbon sheet: (A) twisted by 360°; (B) sheet fabric. Reprinted with permission from ref 46. Copyright 2006 American Chemical Society.

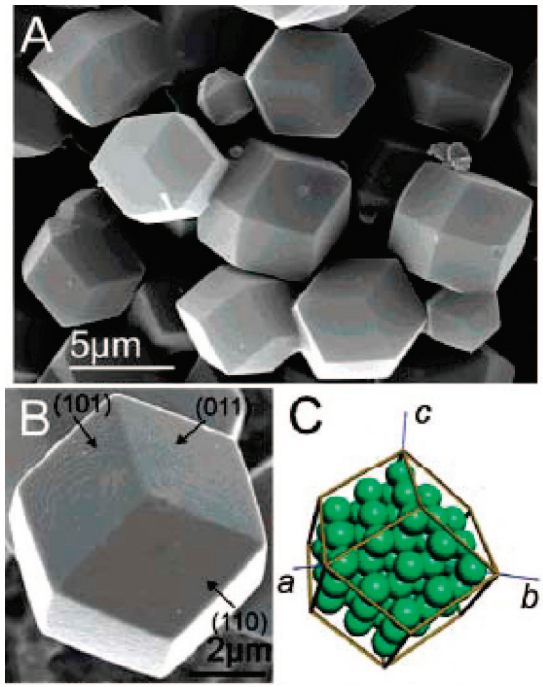

Figure 16. (A, B) SEM images of mesoporous carbon FDU-16. (C) Structural model. Reprinted with permission from ref 70. Copyright 2007 ACS.

can be obtained with a hydrophobic interface. A high temperature may accelerate the polymerization while weakening the hydrogen-bonding reaction, leading to the failure assembly. The low polymerization at a low temperature could not fix the mesostructure. Interestingly, at a given temperature (66 °C) and stirring rate (~300 rpm), large single crystals (~5 μm) of body-centered cubic ($Im\bar{3}m$) mesoporous carbon with a perfect rhombdodecahedral morphology can be obtained (Figure 16).[70] It is highlighted that the medium temperature can balance the assembly and condensation and the medium stirring rate favors the mass transport for the precipitation of large single crystals. It is benefited from the perfect single crystals that a layer-by-layer growth mechanism is proposed for body-centered cubic mesostructure from the centers of 12 {110} planes of the rhombdodecahedral morphology.

Hard-template, such as anodic aluminum oxide (AAO)[71] and colloidal silica,[72,73] assisted fabrication is normally used for fibers and macroporous materials. The confined growth of mesostructures inside the voids from the hard template replicates the macrospaces. Mesoporous carbon wires with the dimensions from 60 to 400 nm can be templated by the AAO membrane.[74] Hierachically ordered macroporous/mesoporous carbons have been obtained from a dual silica colloidal crystal and block copolymer F127 system.[75] Mesopores (~12 nm) are inherited from the decomposition of the triblock copolymer and macropores (312–438 nm) are the replication of voids for 3D face-centered cubic (fcc) colloidal crystal arrays.

6. Hybrid Mesoporous Carbon-Based Materials

Hybrid porous materials with well-defined pore structures and tailored components are of great interests for high performance applications.[76] Heteroatom-containing mesoporous carbon replicas can be directly synthesized by using the carbon source consisting of functional groups, for example, ethylenediamine.[77] In addition, diazonium compound and fluorine gas were found to react with mesoporous carbon and be covalently grafted on carbon.[78–80] However, rigorous conditions may destroy the mesostructure to some extent. It is expected to provide an alternative opportunity for designing functional mesoporous carbons with improving or additional physicochemical properties.

A good example for supramolecular templating hybrid mesoporous solids is functionalized mesoporous silicas in which silane $(R'O)_4Si$ and organosilane $(R'O)_3Si$-R (where R′ is Et or Me and R is a nonhydrolyzable ligand) precursors coassembly with amphiphilic surfactants.[76] The co-condensation of two precursors constructs the matrix. Therefore, the reactivity of the organic precursor such as phenolic resol should be thoroughly considered to prepare hybrid mesoporous carbons.

6.1. Phenolic Resol or Furfuryl Alcohol and Tetraethylorthosilicate (TEOS). The addition of silicates into phenolic resins is widely used in industry to enhance the toughness of polymers and carbons and resist the thermal shrinkage. The functional groups such as hydroxyl, benzyl, and ester groups can fully or partially react with compatible groups (e.g., silanol groups) which are formed from the hydrolysis and condensation of a silicon alkoxide. In

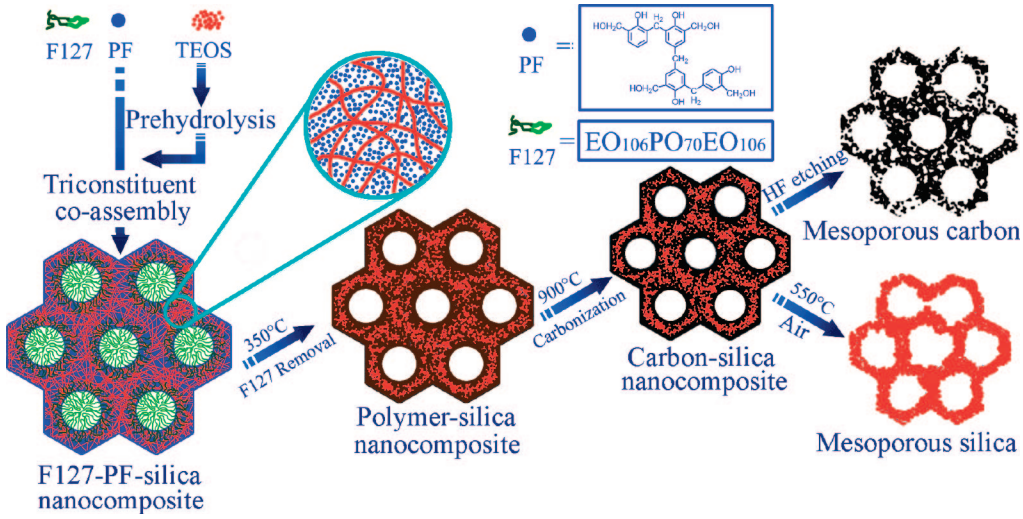

Figure 17. Triconstituent coassembly to ordered mesoporous polymer−silica and carbon−silica nanocomposites, as well as the corresponding ordered mesoporous silica and carbon frameworks. Reprinted with permission from ref 81 Copyright 2006 American Chemical Society.

combination with this knowledge and the supramolecular templating approach, we demonstrated a triconstituent coassembly route in which phenol-formaldehyde resol (a polymer precursor), TEOS (a silica precursor), and a block copolymer are assembled together (Figure 17).[81] This route leads to ordered mesostructures involving a polymer phase, a triblock copolymer template phase, and a silicate phase in a nanocomposite structure. Removal of the template is carried out by calcination similar to the process in the pure phenolic resin networks. The polymer phase can also be carbonized. The products experience less shrinkage than if only a single organic resin phase is presented and possess relatively large mesopores, because the silicate components enhance the rigidity of the nanocomposite frameworks. Notably, the ratio of Si/resin can range from 0 to infinite. A "reinforced concrete" model is proposed to understand the structure of the nanocomposites in which silica and carbon components are microphase separated and "homogenously" dispersed inside the pore walls. Etching with HF or combustion in air can remove silica or carbon components in the carbon−silica nanocomposite to form pure mesoporous carbon and silica, respectively. The former process can build pores in the carbon pore walls, the dimension depending on the size of the silicate oligomers. Highly ordered mesoporous carbon has extremely large surface area (~2400 m^2/g), which is principally contributed from the micropores or small mesoporous left by the etching of silica in the pore walls, and relatively large mesopores (~6.7 nm) which are originated from the mother carbon−silica composite. The large-surface-area mesoporous carbon exhibits good performance in both electrochemical double layer capacitor and adsorption for dyes.

Lin and co-workers separately reported the similar triconstituent coassembly of triblock copolymer, phenolic resin and TEOS in an aqueous solution.[82] An aerosel-assisted route has also been utilized to prepare mesoporous carbon−silica polydispersed particles.[83] Similar phenomena were observed. For example, the nanocomposite after dissolution of silica gives mesostructured carbon and after burning off carbon gives mesostructured silica. Mesoporous carbon has large surface area, almost 5 times higher than the nanocomposite or the mesoporous silica from the same nanocomposite.

Furfuryl alcohol (FA) can copolymerize with silicates during the hydrolysis of TEOS under an acidic condition to produce penetrating carbon−silica hybrid materials.[84] Therefore, a triblock-copolymer templating process can derive PFA−silica mesoporous nanocomposites. However, only wormlike pores were obtained if the organic monomer FA and TEOS were mixed together at the beginning of the synthesis.[85] The uncontrollable polymerization of FA monomer may perturb the self-assembly of block copolymers.

6.2. Phenolic Resol and Titanium Complex. Titanium carbides exhibit high electrical conductivity, high mechanical stiffness, low density, and catalytic activity resembling the metals.[86] The embedment of TiC nanocrystals in the matrix of an amorphous carbon matrixes has been developed to provide an appropriate combination of electrical and mechanical properties.[87,88] A coassembling procedure using titanium citrate, resol, and triblock copolymer Pluronic F127 is developed to synthesize ordered mesoporous nanocrystalline titanium carbide/carbon composites.[89] Both of hydrophilic titanium citrate and resol can be hydrogen-bonded with the triblock copolymer, driving the ordered, self-assembled mesostructure. The titanium and carbon precursors, tinanium citrate and resol, which are involved in the Pechini-like process,[90] enable the cross-linking of polyols (resols) with polycarboxylate chelating to titanium ions through strong intermolecular hydrogen-bonding interaction. This process restricts the aggregation and condensation of Ti−O species[91] as well as the esterification between titanium and phenol hydroxyl group.[92] The formation of titanium oxide nanocrystals at temperature below 600 °C is inhibited and the loss of structural regularity caused by the growth of crystalline titania is avoided before the formation of rigid carbon frameworks. Therefore, curing the composite results in the ordered polymer mesostructure with high content and dispersion of titanium. In situ carbothermal reduction is carried out to generate the TiC nanocrystals in the mesoporous carbon matrix (Figure 18).[89]

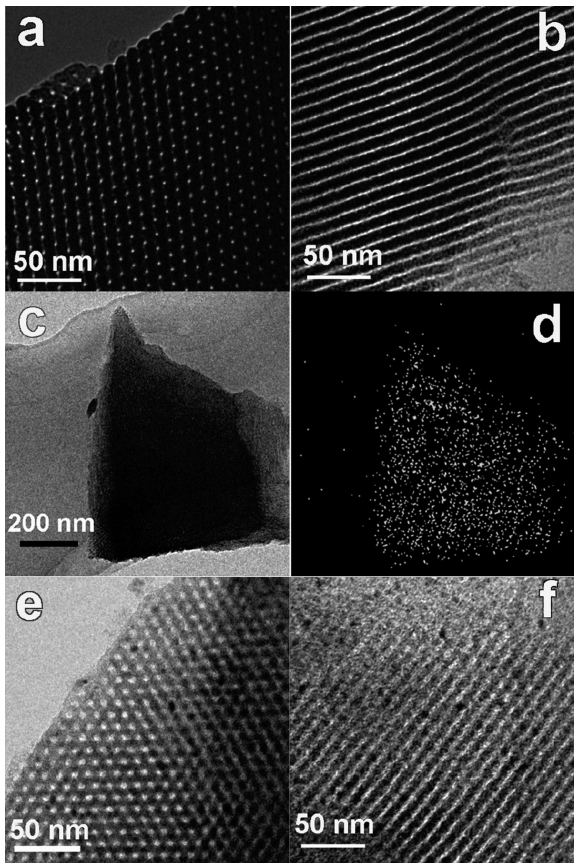

Figure 18. TEM images and energy-dispersive X-ray (EDX) mapping of mesoporous titanium/carbon composites. Images of the sample after carbothermal reduction at 600 °C taken along (a) [001] and (b) [110] directions. (c) Images of particle morphology for the sample and (d) corresponding titanium element face mapping, indicating the high dispersion of titanium element in the carbon matrix. TEM images of the sample after carbothermal reduction at 1000 °C, taken along (e) [001] and (f) [110] directions.

If the alcoholysis product of titanium tetrachloride serves as an inorganic precursor, phenolic resols are used as the organic precursor, triblock copolymer templating approach under strongly acidic conditions would lead to the formation of ordered mesoporous TiO_2-C nanocomposite after pyrolysis at 600 °C.[93]

6.3. Phenol, *p*-Fluorophenol, and Formaldehyde. Fluorinated carbon has long been studied to widen the applications for carbon in high electrical conductors, primary and secondary batteries, electromagnetic materials, and aerospace technology.[79,94] Very recently, we reported the synthesis of highly ordered fluorinated mesoporous carbons by the direct triblock-copolymer-templating approach.[95] The organic precursors are phenol, formaldehyde, and *p*-fluorophenol, which can polymerize to generate soluble phenolic resins modified with fluorine. *p*-Fluorophenol serves as a functional monomer similar to the organic-group-containing alkoxysilane in the synthesis of functionalized mesoporous silicates. Similar to resols, fluorine-containing phenolic resins selectively swell in PEO domain. This domain, together with hydrophobic PPO domain, self-assembles to ordered packed cylinders and spheres, depending on the V_H/V_L ratio. After high-temperature carbonization at 900 °C, highly ordered mesoporous carbon with covalent C−F bonds, high surface areas, and narrow pore sizes can be obtained. The fluorinated mesoporous-carbon-modified electrode exhibits a higher electron-transfer rate than both pure mesoporous carbon modified and bare GC electrodes, showing potentials in electrocatalytic reactions.

7. Conclusions and Outlook

The supramolecular templating approach opens an avenue for ordered mesoporous polymers and carbons and has advantages in large-scale production with bulk amounts. Research is now mostly centered on phenolic resins. Referring to the soft-matter chemistry, the cross-linking feature of organic precursors, and the interaction between templates and precursors, mesoporous polymers and carbons with diverse compositions, symmetries, pore dimensions, and morphologies are expected. The inherent reactive and cross-linking characters of organic oligomers favor the design of this kind of materials. Biocompatible and conductive mesoporous polymeric materials are highly desirable. The design and synthesis also include multifunctional mesoporous carbons, for example, graphitized, conductive and oriented carbons, and ordered arrays of multiwalled carbon nanotubes. Through self-assembly, mesoporous semiconductors with high melting point such as carbides, nitrides, and sulfides are the next goal. Hybrid mesoporous polymer- and carbon-based materials are also of great significance because of the merits from synergistic roles of each component. Besides co-condensation, postgrafting is also an easy route for functionalizing porous materials. Mesoporous polymer resin frameworks that consist of more reacted sites may be more easily functionalized than mesoporous silica. Both routes are open for more fantasy functions. Different from mesoporous silica, the assembling of mesoporous polymeric frameworks can be divided into steps. Consequently, bicontinuous P and D mesophases will be synthesized for mesoporous polymers and carbons, especially when ABC triblock copolymers are involved in the preparation. A thorough structural control should be the future work on the combination of theoretical modeling of the formation mechanism and the experimental synthesis work. All these efforts for ordered mesoporous polymers and carbons are aimed at meeting future technological applications.

Acknowledgment. This work was supported by the NSF of China (20421303, 20407014, and 20521140450), the State Key Basic Research Program of the PRC (2006CB202502 and 2006CB932302), the Shanghai Science & Technology and Education Committee (06DJ14006, 055207078, 07QH14011, and T0402), and Shanghai Nanotech Promotion Center (0652nm024), the Program for New Century Excellent Talents in Universities (NCET-07-0560), and Shanghai Leading Academic Discipline Project (B108). We thank Prof. Stephen T. Hyde for helpful discussion.

References

(1) Whitesides, G. M.; Boncheva, M. *Proc. Natl. Acad. Sci.* **2002**, *99*, 4769.
(2) Kresge, C. T.; Leonowicz, M. E.; Roth, W. J.; Vartuli, J. C.; Beck, J. S. *Nature* **1992**, *359*, 710.
(3) Yanagisawa, T.; Shimizu, T.; Kuroda, K.; Kato, C. *Bull. Chem. Soc. Jpn.* **1990**, *63*, 988.
(4) Hamley, I. W. *Angew. Chem., Int. Ed.* **2003**, *42*, 1692.
(5) Hyde, S. T. Identification of Lyotropic Liquid Crystalline Mesophases. In *Handbook of Applied Surface and Colloid Chemistry*; Holmberg, K., Ed.; John Wiley & Sons: New York, 2001; p 299.
(6) Corma, A. *Chem. Rev.* **1997**, *97*, 2373.

(7) Ying, J. Y.; Mehnert, C. P.; Wong, M. S. *Angew. Chem., Int. Ed.* **1999**, *38*, 56.
(8) Davis, M. E. *Nature* **2002**, *417*, 813.
(9) Wan, Y.; Zhao, D. Y. *Chem. Rev.* **2007**, *107*, 2821.
(10) Beck, J. S.; Vartuli, J. C.; Roth, W. J.; Leonowicz, M. E.; Kresge, C. T.; Schmitt, K. D.; Chu, C. T. W.; Olson, D. H.; Sheppard, E. W.; McCullen, S. B.; Higgins, J. B.; Schlenker, J. L. *J. Am. Chem. Soc.* **1992**, *114*, 10834.
(11) Tanev, P. T.; Pinnavaia, T. J. *Science* **1995**, *267*, 865.
(12) Huo, Q. S.; Margolese, D. I.; Ciesla, U.; Feng, P. Y.; Gier, T. E.; Sieger, P.; Leon, R.; Petroff, P. M.; Schuth, F.; Stucky, G. D. *Nature* **1994**, *368*, 317.
(13) Zhao, D. Y.; Feng, J. L.; Huo, Q. S.; Melosh, N.; Fredrickson, G. H.; Chmelka, B. F.; Stucky, G. D. *Science* **1998**, *279*, 548.
(14) Che, S.; Garcia-Bennett, A. E.; Yokoi, T.; Sakamoto, K.; Kunieda, H.; Terasaki, O.; Tatsumi, T. *Nat. Mater.* **2003**, *2*, 801.
(15) Yang, P. D.; Zhao, D. Y.; Margolese, D. I.; Chmelka, B. F.; Stucky, G. D. *Nature* **1998**, *396*, 152.
(16) Tian, B. Z.; Liu, X. Y.; Tu, B.; Yu, C. Z.; Fan, J.; Wang, L. M.; Xie, S. H.; Stucky, G. D.; Zhao, D. Y. *Nat. Mater.* **2003**, *2*, 159.
(17) Attard, G. S.; Bartlett, P. N.; Coleman, N. R. B.; Elliott, J. M.; Owen, J. R.; Wang, J. H. *Science* **1997**, *278*, 838.
(18) Braun, P. V.; Osenar, P.; Stupp, S. I. *Nature* **1996**, *380*, 325.
(19) Wan, Y.; Yang, H. F.; Zhao, D. Y. *Acc. Chem. Res.* **2006**, *39*, 423.
(20) Kyotani, T. *Bull. Chem. Soc. Jpn.* **2006**, *79*, 1322.
(21) Lee, J.; Kim, J.; Hyeon, T. *Adv. Mater.* **2006**, *18*, 2073.
(22) Bates, F. S.; Fredrickson, G. H. *Phys. Today* **1999**, *52*, 32.
(23) Hillmyer, M. A. Nanoporous materials from block copolymer precursors. In *Block Copolymers II*; Springer-Verlag: Berlin, 2005; Vol. 190, p 137.
(24) Lu, A. H.; Li, W. C.; Salabas, E. L.; Spliethoff, B.; Schuth, F. *Chem. Mater.* **2006**, *18*, 2086.
(25) Lu, A. H.; Schuth, F. *Adv. Mater.* **2006**, *18*, 1793.
(26) Yang, H. F.; Zhao, D. Y. *J. Mater. Chem.* **2005**, *15*, 1217.
(27) Ryoo, R.; Joo, S. H.; Jun, S. *J. Phys. Chem. B* **1999**, *103*, 7743.
(28) Lee, J.; Yoon, S.; Hyeon, T.; Oh, S. M.; Kim, K. B. *Chem. Commun.* **1999**, 2177.
(29) Al-Muhtaseb, S. A.; Ritter, J. A. *Adv. Mater.* **2003**, *15*, 101.
(30) Gao, C. B.; Sakamoto, Y.; Sakamoto, K.; Terasaki, O.; Che, S. N. *Angew. Chem., Int. Ed.* **2006**, *45*, 4295.
(31) Zhang, F. Q.; Meng, Y.; Gu, D.; Yan, Y.; Yu, C. Z.; Tu, B.; Zhao, D. Y. *J. Am. Chem. Soc.* **2005**, *127*, 13508.
(32) Epps, T. H.; Cochran, E. W.; Hardy, C. M.; Bailey, T. S.; Waletzko, R. S.; Bates, F. S. *Macromolecules* **2004**, *37*, 7085.
(33) Meng, Y.; Gu, D.; Zhang, F. Q.; Shi, Y. F.; Yang, H. F.; Li, Z.; Yu, C. Z.; Tu, B.; Zhao, D. Y. *Angew. Chem., Int. Ed.* **2005**, *44*, 7053.
(34) Moriguchi, I.; Ozono, A.; Mikuriya, K.; Teraoka, Y.; Kagawa, S.; Kodama, M. *Chem. Lett.* **1999**, 1171.
(35) Li, Z. J.; Yan, W. F.; Dai, S. *Carbon* **2004**, *42*, 767.
(36) Lee, K. T.; Oh, S. M. *Chem. Commun.* **2002**, 2722.
(37) Nishiyama, N.; Zheng, T.; Yamane, Y.; Egashira, Y.; Ueyama, K. *Carbon* **2005**, *43*, 269.
(38) Wan, Y.; Shi, Y. F.; Zhao, D. Y. *Chem. Commun.* **2007**, 897.
(39) Lipic, P. M.; Bates, F. S.; Hillmyer, M. A. *J. Am. Chem. Soc.* **1998**, *120*, 8963.
(40) Kosonen, H.; Ruokolainen, J.; Nyholm, P.; Ikkala, O. *Macromolecules* **2001**, *34*, 3046.
(41) Kosonen, H.; Valkama, S.; Nykanen, A.; Toivanen, M.; ten Brinke, G.; Ruokolainen, J.; Ikkala, O. *Adv. Mater.* **2006**, *18*, 201.
(42) Valkama, S.; Ruotsalainen, T.; Nykanen, A.; Laiho, A.; Kosonen, H.; ten Brinke, G.; Ikkala, O.; Ruokolainen, J. *Macromolecules* **2006**, *39*, 9327.
(43) Valkama, S.; Nykanen, A.; Kosonen, H.; Ramani, R.; Tuomisto, F.; Engelhardt, P.; ten Brinke, G.; Ikkala, O.; Ruokolainen, J. *Adv. Funct. Mater.* **2007**, *17*, 183.
(44) Soininen, A.; Valkama, S.; Nykanen, A.; Laiho, A.; Kosonen, H.; Mezzenga, R.; Ruokolainen, J. *Chem. Mater.* **2007**, *19*, 3093.
(45) Liang, C. D.; Hong, K. L.; Guiochon, G. A.; Mays, J. W.; Dai, S. *Angew. Chem., Int. Ed.* **2004**, *43*, 5785.
(46) Liang, C. D.; Dai, S. *J. Am. Chem. Soc.* **2006**, *128*, 5316.
(47) Tanaka, S.; Nishiyama, N.; Egashira, Y.; Ueyama, K. *Chem. Commun.* **2005**, 2125.
(48) Liu, C. Y.; Li, L. X.; Song, H. H.; Chen, X. H. *Chem. Commun.* **2007**, 757.
(49) Meng, Y.; Gu, D.; Zhang, F. Q.; Shi, Y. F.; Cheng, L.; Feng, D.; Wu, Z. X.; Chen, Z. X.; Wan, Y.; Stein, A.; Zhao, D. Y. *Chem. Mater.* **2006**, *18*, 4447.
(50) Huang, Y.; Cai, H. Q.; Yu, T.; Zhang, F. Q.; Zhang, F.; Meng, Y.; Gu, D.; Wan, Y.; Sun, X. L.; Tu, B.; Zhao, D. Y. *Angew. Chem., Int. Ed.* **2007**, *46*, 1089.
(51) Deng, Y. H.; Yu, T.; Wan, Y.; Shi, Y. F.; Meng, Y.; Gu, D.; Zhang, L. J.; Huang, Y.; Liu, C.; Wu, X. J.; Zhao, D. Y. *J. Am. Chem. Soc.* **2007**, *129*, 1690.
(52) Zhou, J. H.; He, J. P.; Ji, Y. J.; Dang, W. J.; Liu, X. L.; Zhao, G. W.; Zhang, C. X.; Zhao, J. S.; Fu, Q. B.; Hu, H. P. *Electrochim. Acta* **2007**, *52*, 4691.
(53) Yu, K.; Smarsly, B.; Brinker, C. J. *Adv. Funct. Mater.* **2003**, *13*, 47.
(54) Mortensen, K.; Brown, W.; Jorgensen, E. *Macromolecules* **1994**, *27*, 5654.
(55) Alexandridis, P.; Olsson, U.; Lindman, B. *Langmuir* **1998**, *14*, 2627.
(56) Forster, S.; Antonietti, M. *Adv. Mater.* **1998**, *10*, 195.
(57) Zhang, F. Q.; Meng, Y.; Gu, D.; Yan, Y.; Chen, Z. X.; Tu, B.; Zhao, D. Y. *Chem. Mater.* **2006**, *18*, 5279.
(58) Pindzola, B. A.; Jin, J. Z.; Gin, D. L. *J. Am. Chem. Soc.* **2003**, *125*, 2940.
(59) Ding, J. H.; Gin, D. L. *Chem. Mater.* **2000**, *12*, 22.
(60) Jenekhe, S. A.; Chen, X. L. *Science* **1999**, *283*, 372.
(61) Lee, J. S.; Hirao, A.; Nakahama, S. *Macromolecules* **1988**, *21*, 274.
(62) Zalusky, A. S.; Olayo-Valles, R.; Wolf, J. H.; Hillmyer, M. A. *J. Am. Chem. Soc.* **2002**, *124*, 12761.
(63) Rzayev, J.; Hillmyer, M. A. *J. Am. Chem. Soc.* **2005**, *127*, 13373.
(64) Bang, J.; Kim, S. H.; Drockenmuller, E.; Misner, M. J.; Russell, T. P.; Hawker, C. J. *J. Am. Chem. Soc.* **2006**, *128*, 7622.
(65) Kowalewski, T.; Tsarevsky, N. V.; Matyjaszewski, K. *J. Am. Chem. Soc.* **2002**, *124*, 10632.
(66) Leiston-Belanger, J. M.; Penelle, J.; Russell, T. P. *Macromolecules* **2006**, *39*, 1766.
(67) Ho, R. M.; Wang, T. C.; Lin, C. C.; Yu, T. L. *Macromolecules* **2007**, *40*, 2814.
(68) Zhao, D. Y.; Sun, J. Y.; Li, Q. Z.; Stucky, G. D. *Chem. Mater.* **2000**, *12*, 275.
(69) Yan, Y.; Zhang, F. Q.; Meng, Y.; Tu, B.; Zhao, D. Y. *Chem. Commun.* **2007**, 2867.
(70) Zhang, F.; Gu, D.; Yu, T.; Zhang, F.; Xie, S.; Zhang, L.; Deng, Y.; Wan, Y.; Tu, B.; Zhao, D. *J. Am. Chem. Soc.* **2007**, *129*, 7746.
(71) Lu, Q. Y.; Gao, F.; Komarneni, S.; Mallouk, T. E. *J. Am. Chem. Soc.* **2004**, *126*, 8650.
(72) Johnson, S. A.; Ollivier, P. J.; Mallouk, T. E. *Science* **1999**, *283*, 963.
(73) Stein, A.; Schroden, R. C. *Curr. Opin. Solid State Mater. Sci.* **2001**, *5*, 553.
(74) Steinhart, M.; Liang, C. D.; Lynn, G. W.; Gosele, U.; Dai, S. *Chem. Mater.* **2007**, *19*, 2383.
(75) Deng, Y.; Liu, C.; Yu, T.; Liu, F.; Zhang, F.; Wan, Y.; Zhang, L.; Wang, C.; Tu, B.; Webley, P. A.; Wang, H.; Zhao, D. *Chem. Mater.* **2007**, *19*, 3271.
(76) Stein, A.; Melde, B. J.; Schroden, R. C. *Adv. Mater.* **2000**, *12*, 1403.
(77) Vinu, A.; Ariga, K.; Mori, T.; Nakanishi, T.; Hishita, S.; Golberg, D.; Bando, Y. *Adv. Mater.* **2005**, *17*, 1648.
(78) Li, Z. J.; Dai, S. *Chem. Mater.* **2005**, *17*, 1717.
(79) Li, Z. J.; Del Cul, G. D.; Yan, W. F.; Liang, C. D.; Dai, S. *J. Am. Chem. Soc.* **2004**, *126*, 12782.
(80) Toupin, M.; Belanger, D. *J. Phys. Chem. C* **2007**, *111*, 5394.
(81) Liu, R. L.; Shi, Y. F.; Wan, Y.; Meng, Y.; Zhang, F. Q.; Gu, D.; Chen, Z. X.; Tu, B.; Zhao, D. Y. *J. Am. Chem. Soc.* **2006**, *128*, 11652.
(82) Lin, H. P.; Chang-Chien, C. Y.; Tang, C. Y.; Lin, C. Y. *Microporous Mesoporous Mater.* **2006**, *93*, 344.
(83) Hu, Q. Y.; Kou, R.; Pang, J. B.; Ward, T. L.; Cai, M.; Yang, Z. Z.; Lu, Y. F.; Tang, J. *Chem. Commun.* **2007**, 601.
(84) Muller, H.; Rehak, P.; Jager, C.; Hartmann, J.; Meyer, N.; Spange, S. *Adv. Mater.* **2000**, *12*, 1671.
(85) Yao, J. F.; Wang, H. T.; Chan, K. Y.; Zhang, L. X.; Xu, N. P. *Microporous Mesoporous Mater.* **2005**, *82*, 183.
(86) Hwu, H. H.; Chen, J. G. G. *Chem. Rev.* **2005**, *105*, 185.
(87) Voevodin, A. A.; Prasad, S. V.; Zabinski, J. S. *J. Appl. Phys.* **1997**, *82*, 855.
(88) Lewin, E.; Wilhelmsson, O.; Jansson, U. *J. Appl. Phys.* **2006**, 100.
(89) Yu, T.; Deng, Y.; Wang, L.; Liu, R. L.; Zhang, L. J.; Tu, B.; Zhao, D. Y. *Adv. Mater.* **2007**, *19*, 2301.
(90) Cushing, B. L.; Kolesnichenko, V. L.; O'Connor, C. J. *Chem. Rev.* **2004**, *104*, 3893.
(91) Kemmitt, T.; Al-Salim, N. I.; Gainsford, G. J.; Bubendorfer, A.; Waterland, M. *Inorg. Chem.* **2004**, *43*, 6300.
(92) Fornasieri, G.; Rozes, L.; Le Calve, S.; Alonso, B.; Massiot, D.; Rager, M. N.; Evain, M.; Boubekeur, K.; Sanchez, C. *J. Am. Chem. Soc.* **2005**, *127*, 4869.
(93) Liu, R. L.; Ren, Y. J.; Shi, Y. F.; Zhang, L. J.; Tu, B.; Zhao, D. Y. *Chem. Mater.* **2007**, DOI: 10.1021/cm071470W.
(94) Nakajima, T.; Li, J. L.; Naga, K.; Yoneshima, K.; Nakai, T.; Ohzawa, Y. *J. Power Sources* **2004**, *133*, 243.
(95) Wan, Y.; Qian, X. F.; Jia, N. Q.; Wang, Z. Y.; Li, H. X.; Zhao, D. Y. *Chem. Mater.* **2007**, DOI: 10.1021/cm071490Y.

CM7024125